FATIGUE BEHAVIOUR AT ROOM TEMPERATURE OF A METAL FOAM BASED EXHAUST AFTERTREATMENT SYSTEM FOR PASSENGER CARS

S. Karditsas[1], G. Savaidis[1], G. Koltsakis[2], Z. Samaras[2]

1. *Laboratory of Machine Elements and Machine Design, Mechanical Engineering Department, Aristotle University of Thessaloniki, Greece*
2. *Laboratory of Applied Thermodynamics, Mechanical Engineering Department, Aristotle University of Thessaloniki, Greece*

ABSTRACT

Experimental results regarding the fatigue behaviour of metal foam based exhaust aftertreatment systems for passenger cars are discussed. Different prototypes were tested under fully reversed cyclic loading with variable acceleration amplitudes at room temperature and a constant frequency of 180 Hz. The cyclic tests exhibited the overall mechanical response of the specimens to fatigue loading, especially the relations between the drive acceleration and the accelerations acting at various positions of the specimens, and identified the failure critical elements.

KEYWORDS: Fatigue, Exhaust systems, Accelerations

1. INTRODUCTION

The main components of a metal foam filter are the metal foam layers, the fiber material and the perforated tube. The most significant component is the metal foam that filters the soot particles of the exhaust-gas. The metal foam has pores and their size may vary from point to point on the same filter. The fiber is made of materials that allow the size changes of the foam due to the temperature changes (contraction-expansion). The perforated tube is made of steel and the foam layers are mounted around it. The metal foam filters, operate at a range of temperature from 100 ^{o}C to 650 ^{o}C for Diesel, and 300 ^{o}C to 1100 ^{o}C for Gasoline. The loads that applied are coming from the oscillations that caused by the exhaust-gas that flows through the filters, the operation of the car engine and the irregularity (roughness) of the roads.

Therefore, the most common method to evaluate the durability of filter prototypes is the hot vibration test (also called, more casually, the “hot shake test”). Most of vehicle manufacturers have their internal specifications for such tests /1/. Generally, the filter is placed on a vibration table of controlled vibration acceleration and frequency. Hot gas of controlled temperature flows through the filter during the test. Hot vibration is a destructive test, where the filter integrity and the extent and nature of damage are evaluated after a prescribed test time. Nevertheless, the present investigation was conducted at room temperature, approximately 20^{o} C, and constitutes a primal step regarding the investigation of the fatigue behavior of metal foams based exhaust aftertreatment systems for passenger cars.

2. SPECIMENS UNDER INVESTIGATION

Three prototype specimens designed for diesel passenger cars were tested, see figure 1. They have not as yet been used in the market. They are designated with the following code specifications:

- Prototype 5
- Korean 12132
- Prototype 2

Figure 1: Specimens under investigation.

Figure 2 shows a 3D-CAD cross-section of the three specimens revealing their composition parts. Prototype 5 consists of the perforated tube, the metal foam, the fiber material, a diaphragm and the steel shell. The diaphragm separates the specimen in two areas, 1 and 2. The length of the first area amounts to 200 mm while the second one amounts to 100 mm. Prototype 2 consists of the same parts except from the diaphragm. Korean 12132 contains additionally a metal net around the metal foam and two thin metal covers (flanges) at the two sides of the foam for extra protection of the foam. An apostate supports the assembly of all the previous mentioned parts to the steel shell. The length of the perforated tubes of Prototype 5 and Prototype 2 amounts to 300 mm and their diameters are 50 mm and 40 mm, respectively. The perforated tube of Korean 12132 is 250 mm long and has a diameter of 50 mm. Prototype 5 and Prototype 2 have a capacity of 2.5 litres, whereas Korean 12132 has a capacity of 1.4 litres.

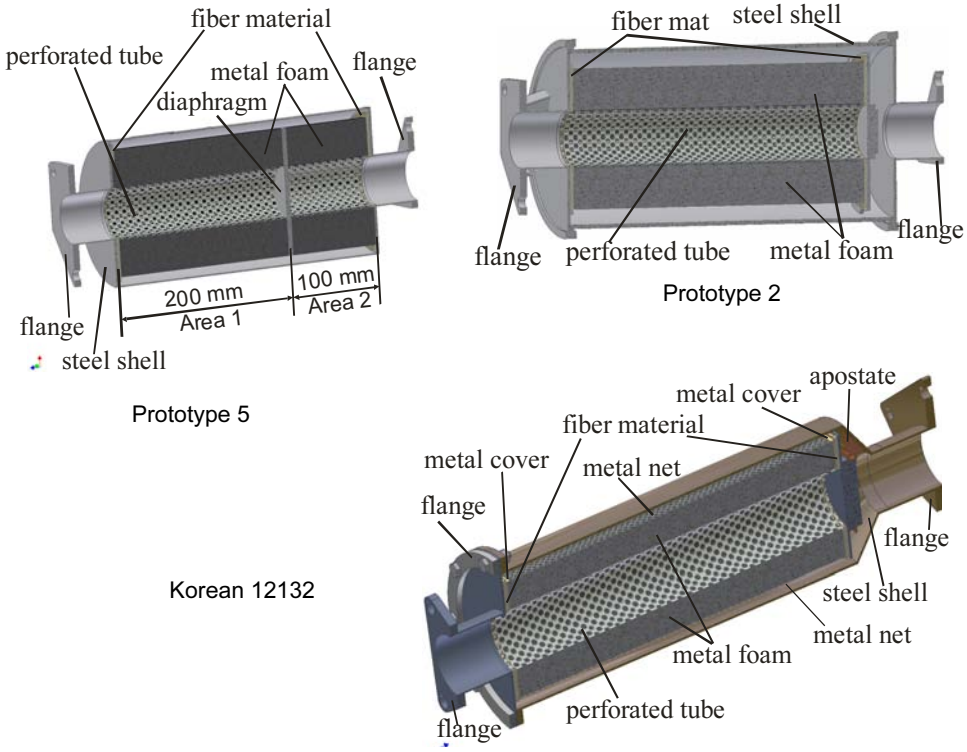

Figure 2: 3D-CAD cross-section of the three specimens.

3. EXPERIMENTAL APPARATUS AND MEASUREMENT TECHNIQUE

Figure 3 shows a 3D-CAD-drawing of the test with Prototype 5 and construction details used for the load introduction in all cases.

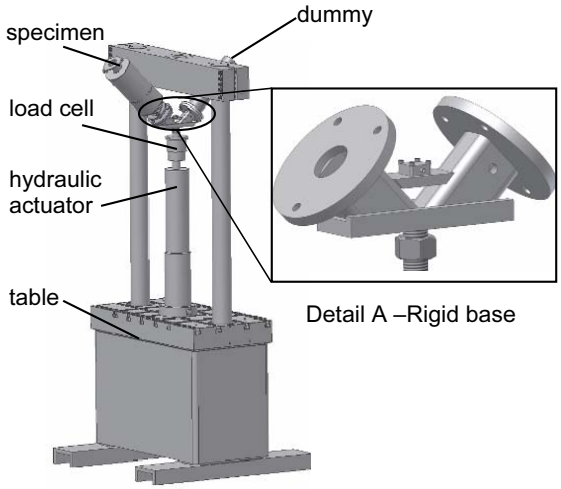

Figure 3: Test rig drawing and construction details.

A hydraulic actuator has been used to introduce the loads to the specimen via a rigid metallic base, which is fixed into the load cell on the actuator's front side; see Detail A in figure 3. Note that the rigid base allows the fixation of two specimens under an angle of 45° each, relative to the load (vertical) axis. Therewith, simultaneous testing of two identical specimens under equal loading conditions is possible. However, since the three specimens were not identical in terms of construction, mass, and centre of gravity, they have been tested separately, whereby appropriate dummies have been manufactured and mounted on the position of the second specimen in order to avoid uncontrolled bending caused by the specimen's mass to the actuator's piston.

Every specimen experiences a biaxial cyclic loading because the external load is introduced vertically to the specimen positioned at 45 degrees relative to the vertical axis. As shown in figure 4, the applied load can be resolved into two equal components acting parallel and perpendicular to the specimen axis.

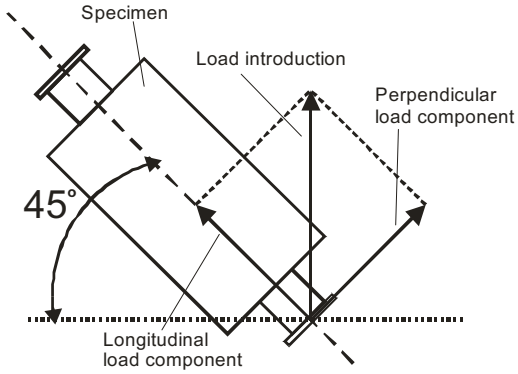

Figure 4: Schematic view of the biaxial cyclic load configuration.

Two identical accelerometers (acceleration range ± 50 m/s^2) were used to control the acceleration of the actuator, which corresponds to the drive signal for the tests and determine the accelerations at various positions of the specimens. Therefore, one accelerometer was mounted on the rigid base of the test rig, which is named position A (figure 5). Figure 6 illustrates the positions of the second accelerometer on the specimens. It has been mounted onto the tube of the specimens, at the position before the perforated tube, named as position B. Therewith, the acceleration acting at the metallic, rigid part near to the position of the introduction of the load could be determined.

In the case of Prototype 5, the second accelerometer was removed after the step-by-step test and mounted on the foam at a distance of approx. 200 mm measured from the gas outlet. This position, named as position C, corresponds to the middle of the area between the gas inlet and the diaphragm; see figure 6. For this purpose, a small part of the steel shell of the specimen was cut to access the metal foam.

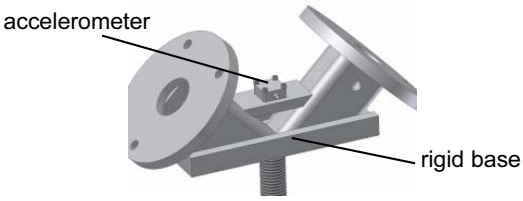

Figure 5: Accelerometer position A on the rigid base.

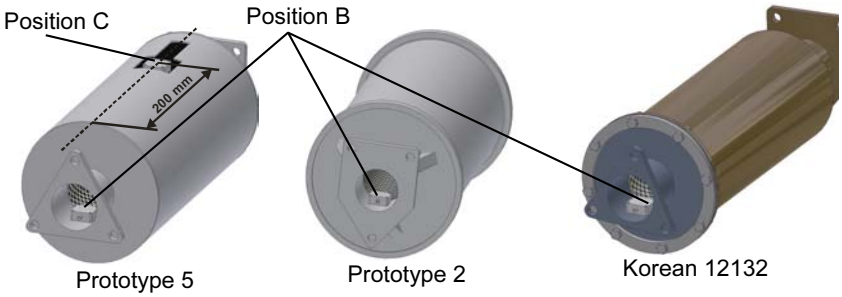

Figure 6: Accelerometer positions B and C.

4. TEST PROGRAM

Two tests have been successively applied to each specimen, specified as:

- Step-by-step test, and
- Durability test.

Within the step-by-step test, constant amplitude loading sequences at four successively increased loading levels (i.e. actuator's acceleration values of ± 50 m/s^2, ± 100 m/s^2, ± 200 m/s^2 and ± 300 m/s^2) have been applied to the specimens. Thereby, the amplitude of the actuator's displacement varied at each loading step. The frequency was kept constant at 180 Hz. Each loading step lasted one hour. Acquisition data were recorded in order to determine the relation between the drive and the measured acceleration signals.

After finishing the step-by-step test, each specimen has been subjected to an additional durability test. Thereby, both the actuator's acceleration and frequency remained constant at ±300 m/s^2 and 180 Hz, respectively. The durability tests lasted till up to the failure of the specimens.

Acceleration data were recorded every 5 minutes for a time range of 20 seconds. The measured acceleration-time signals and the Power Density Spectra have been on-line evaluated in order to control the test and to obtain possible indications relating to damage or even failure of the specimen.

5. RESULTS

5.1 Step-by-step test

Figures 7 and 8 show exemplary typical acceleration signals measured simultaneously at positions A and B (A: actuator's output, position B: perforated tube) and at positions A and C (position C: foam), respectively, during loading step 1 of Prototype 5 over a time range of 0.5 sec. Details regarding the peak values, the waveform and the frequency of the acceleration signals can be obtained from them.

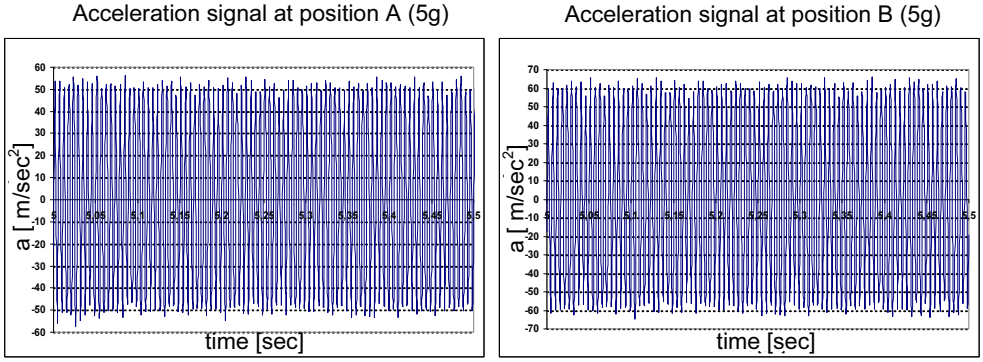

Figure 7: Typical acceleration signals measured at positions A (left side) and B (right side) for a time range of 0.5 sec during loading step 1 of Prototype 5.

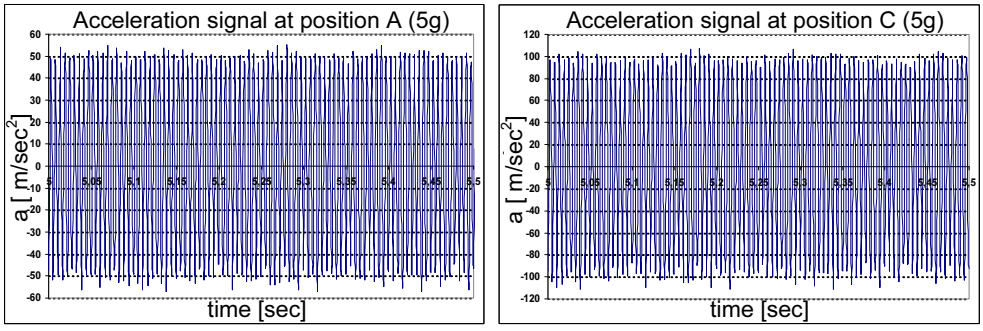

Figure 8: Typical acceleration signals measured at positions A (left side) and C (right side) for a time range of 0.5 sec during loading step 1 of Prototype 5.

Tables 1, 2 and 3 summarize the acquired acceleration values achieved during the step-by-step test as well as the relations derived from it for the specimens Prototype 5, Korean 12132 and Prototype 2.

Table 1: Accelerations obtained during the step-by-step test of Prototype 5.

Loading step	Acceleration value [m/s^2] at Position			Acceleration ratio	
	A	B	C	a_B/a_A	a_C/a_A
1	50	60	100	1.2	2
2	100	120	200	1.2	2
3	200	240	450	1.2	2.25
4	300	400	700	1.3	2.3

Similar signals were measured during the other loading steps of all specimens. The corresponding relations between the acceleration values were determined. No worth-mentioning changes of the measured signals could be observed.

Regarding Prototype 5, an approximately constant relation between the acceleration values at the positions A and B can be derived as $a_B / a_A \approx 60/50 = 1.2$. The relation between the acceleration values at positions A and C amounts to $a_C / a_A \approx 100/50 = 2$.

In the case of Korean 12132 the second accelerometer was mounted only at position B (perforated tube).

The accelerations acting at the beginning of the perforated tube of the Korean 12132 are 1.2 to 1.3 times higher than the ones output from the actuator.

Table 2: Accelerations obtained during the step-by-step test of Korean 12132.

Loading step	Acceleration [m/s^2] at Position		Acceleration ratio
	A	B	a_B/a_A
1	50	60	1.2
2	100	120	1.2
3	200	240	1.2
4	300	400	1.3

Regarding Prototype 2, it is apparent, that the beginning of the perforated tube (position B) experiences accelerations that are 1.27 to 1.45 times higher than the ones output from the actuator.

Table 3: Accelerations obtained during the step-by-step test of Prototype 2.

Loading step	Acceleration [m/s^2] at Position		Acceleration ratio
	A	B	a_B/a_A
1	55	75	1.27
2	105	150	1.33
3	220	320	1.45
4	320	475	1.40

Fast-Fourier-Transformation on-line analyses of the measured signals yield the Power Density Spectra (PDS). Characteristic PDS shown in figure 9 confirm the only existent frequency of the excitation signal of 180 Hz.

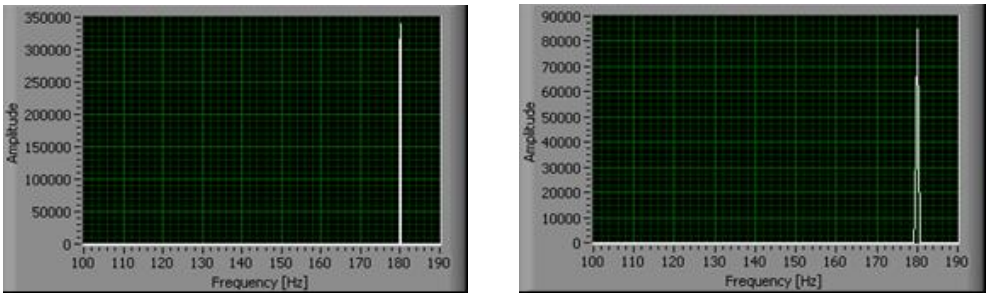

Figure 9: Power Density Spectra derived from FFT-analyses of the acceleration signals measured at positions A (left side) and B (right side) during loading step 1 of step-by-step test of Prototype 5.

5.2 DURABILITY TEST

After finishing the step-by-step tests, inspections of the three specimens were performed. No visible damage could be detected. The specimens have then been subjected to the durability test.

5.2.1 Prototype 5

After approximately 30 minutes of testing, small pieces of the fiber material were cut out and fell out of the tube of the specimen. Nevertheless, the test has been further carried out.

After 2 hours of testing, the perforated tube was also damaged. The red arrows in figure 10 points out the damage position near the gas inlet and the type of damage (total fracture along the periphery of the tube).

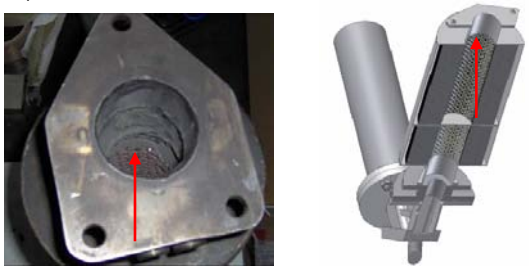

Figure 10: Failure position of prototype 5 after 2 hours.

5.2.2 Korean 12132

After approximately 10 minutes of testing, a visible vaporization of the fiber took place. This phenomenon lasted for approximately 1 hour. Though an immediate inspection has not been performed, it can be assumed that the fiber was completely removed after 1 hour.
Two welds of the tube failed after a total time of 2.5 and 9.5 hours, respectively. In both cases the tube was re-welded in order to curry out the durability test. In the first case, the specimen disassembled and inspected. Figure 11 shows the disassembled specimen. The total absence of the fiber could be confirmed.

Finally, after a total testing time of 21 hour, the perforated tube was damaged, exhibiting a similar fracture behavior as the one observed at prototype 5, i.e. total fracture of the perforated tube. Figure 12 shows the total fracture of the perforated tube in the region close to the gas inlet.

No damage of the foam of Korean 12132 could be observed.

Figure 11: The disassembling of specimen after 2.5 hours confirmed absence of the fiber.

Figure 12: Failure of the perforated tube of Korean 12132 after 21 hours.

5.2.3 Prototype 2

After approximately 3 hours of testing, the specimen was disassembled and inspected. The fiber material has been wearied out. Small pieces of the fiber material were cut out and fell into the steel shell of the specimen. Nevertheless, the test has been further carried out.
After 10 hours of testing the specimen was disassembled and inspected again. The fiber mat and the foam were able to revolve around the perforated tube.
After 18.5 hours of testing, the perforated tube of the specimen was damaged. The red arrow in Figure 13 points out the damage position near the gas inlet and the type of damage (total fracture along the periphery of the tube). Because of the failure of the perforated tube, two or three foam layers near to failure position were damaged. The fiber material was not totally damaged, see figure 13.

Figure 13: Failure position of prototype 2 after 18.5 hours.

6. CONCLUSIONS

Three specimens (Prototype 5, Korean 12132 and Prototype 2) have been subjected to fully-reversed cyclic loading to reveal the fatigue behavior and the failure critical parts at room temperature. First, a step-by-step test consisting of four different loading steps with various magnitudes of acceleration was applied on each specimen while the frequency was kept constant at 180 Hz. Then, a constant amplitude loading sequence (actuator's acceleration = $\pm$ 300m/s^2) has been applied till up to the failure of each specimen.

All accelerations signals measured during both test programs exhibit qualitatively similar waveforms. On-line FFT analyses confirmed that the frequency of the measured signals remained constant at 180 Hz over the whole duration of the tests whereas no indications relating to damage or failure of the specimens were obtained.

During the step-by-step tests the relations between the drive signal (actuator's acceleration) and the acceleration signals measured at the certain positions on the specimens were determined. The relation between two positions at each specimen was nearly constant without regard to the different acceleration values that applied during each loading step. In cases of Prototype 5 and Korean 12132 an approximately constant relation between the acceleration values at the positions A and B was derived as $a_B / a_A \approx 60/50 = 1.2$ whereas this relation regarding Prototype 2 is approximately 1.35. In case of Prototype 5 the relation between the acceleration values at positions A and C amounts to $a_C / a_A \approx 100/50 = 2$.

The durability tests point out that the critical spots of all the specimens in regard to failure are the transition areas from the non-perforated to the perforated part of the tube either near to the gas inlet (Prototype 2 and Korean 12132) or near to the gas outlet (Prototype 5).

The fiber material is the first component providing damage and reducing the stiffness of the specimens. The metal foam wasn't damaged except from the case of Prototype 2 where two or three inner foam layers near to failure position were damaged.

The results of the tests can be used by the manufacturers for evaluation of the filter integrity and the extent and nature of damage in order to make the necessary modifications, i.e. to increase the strength of the perforated tube by enforcing the critical spots.

7. REFERENCES

1. DieselNet Technology Guide, "Catalytic Converters", www.DieselNet.com. Copyright © Ecopoint Inc. Revision 2004.03, 03/06/2008.